PHASE SEPARATION AND INSULATOR-METAL BEHAVIOR OF CMR MANGANITES

The doped manganites, $R_{1-x}Ca_xMnO_3$, where R is a trivalent rare-earth metal, have a distorted-perovskite structure with three-dimensional networks of the MnO_6 octahedra. Their generic behavior of paramagnetic-to-ferromagnetic transition is understood within the framework of double-exchange theory. We need to consider additional effects in order to understand the insulator-metal behavior as well as the colossal magnetoresistance (CMR). At present, the most probable candidate is the *percolation* model [1], in which the insulator-metal behavior occurs when the percolation pass of the metallic (ferromagnetic metallic; FM) is connected from one end to the other regions in the sea of the insulating (charge-ordered insulating; COI) state. The charge-ordering transition of doped manganites usually accompanies an antiferromagnetic transition with the CE-type structure, while the FM state is of half-metallic. Here, to judge the suitability of this model, we have performed a synchrotron radiation X-ray powder diffraction experiment on $Nd_{0.55}(Sr_{1-y}Ca_y)_{0.45}MnO_3$ at beamline **BL02B2** with high angular resolution and counting statistics [2].

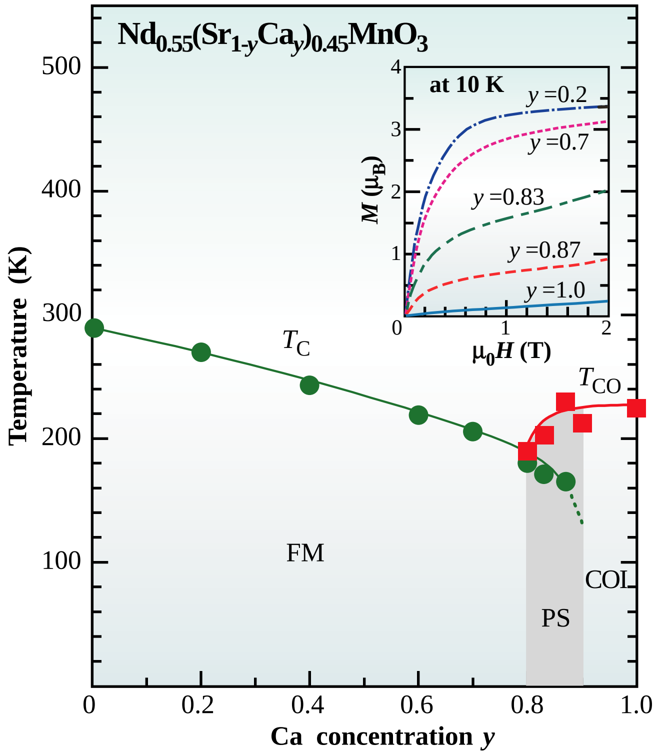

Fig. 1. Electronic phase diagram of $Nd_{0.55}(Sr_{1-y}Ca_y)_{0.45}MnO_3$. COI, FM and PS represent the charge-ordered insulating, ferromagnetic metallic and phase-separated states, respectively. Inset shows magnetization curves at 10 K.

To choose an appropriate chemical composition for the present study, we first have synthesized a series of ceramics $Nd_{0.55}(Sr_{1-y}Ca_y)_{0.45}MnO_3$, finely controlling the one-electron bandwidth through chemical pressure. Powder X-ray diffraction measurements at room temperature along with Rietveld analysis indicate that the samples were single phase without detectable impurities. Figure 1 shows an electronic phase diagram of $Nd_{0.55}(Sr_{1-y}Ca_y)_{0.45}MnO_3$. The Curie temperature T_C and the charge-ordering temperature T_{CO} were determined from the temperature-variation of the magnetization M and resistivity ρ. The insulator-metal behavior was enhanced in the proximity of FM-COI phase boundary (hatched region of Fig. 1). Thus, we have chosen $Nd_{0.55}(Sr_{0.17}Ca_{0.83})_{0.45}MnO_3$ for present investigation. The inset shows the magnetization curves measured at 10 K. The suppressed magnetization curve at 0.83 suggests a coexistence of the FM and antiferromagnetic COI phases [3].

In Fig. 2, we demonstrate prototypical examples of the X-ray powder diffraction patterns of $Nd_{0.55}(Sr_{0.17}Ca_{0.83})_{0.45}MnO_3$ at 265 K and 110 K. At 110 K we observed remarkable splitting of the Bragg reflections, indicating the phase separation (see inset of Fig. 2(b)). We have analyzed the powder patterns below 200 K using a two-phase model with two distorted-perovskites (*Pbnm*; Z = 4). The Rietveld refinements are satisfactory, in which R_{wp} and R_I (reliable factor based on the integrated intensities) are fairly typical of published structures. These two perovskite phases can be characterized by a lattice constant c. Hereafter, we will refer to the respective phases as 'short-c' (7.54 - 7.58 Å) and 'long-c' (7.60 - 7.62 Å) phases.

Figure 3 shows temperature variation of (a) resistivity ρ, (b) lattice constants and (c) intensity of the magnetic Bragg reflections of $Nd_{0.55}(Sr_{0.17}Ca_{0.83})_{0.45}MnO_3$. The most important point here is that the lattice constants indicate a discontinuous change at T_{CO}. In other words, the system is transformed into a two-phase state, *both of which differ from the room temperature phase*. Such a state is perhaps ascribed to the random nucleation of a low-temperature phase and subsequent stress-induced growth of the secondary phase (*stress-induced phase separation*). With further temperature decrease, an insulator-metal transition takes place at 157 K (= T_{IM}).

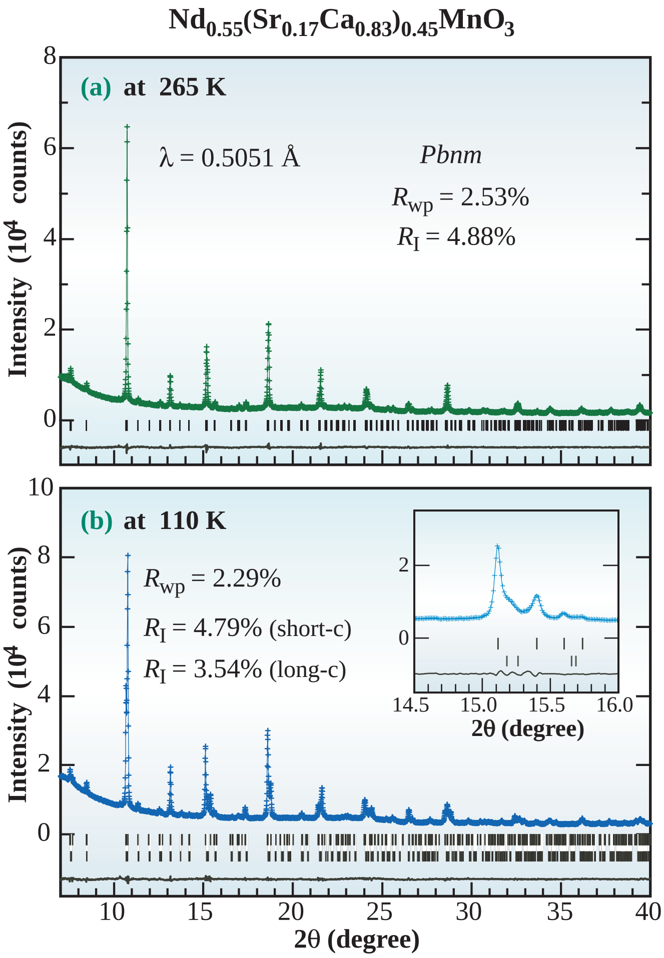

Fig. 2. X-ray powder diffraction patterns (crosses) of $Nd_{0.55}(Sr_{0.17}Ca_{0.83})_{0.45}MnO_3$ at ***(a)*** *265 K and* ***(b)*** *110 K. The solid curve is the result of the Rietveld analysis with a model for* ***(a)*** *single distorted-perovskite (Pbnm; Z = 4) and* ***(b)*** *two distorted-perovskites, respectively.*

The bottom panel of Fig. 3 shows integrated intensities of the magnetic Bragg reflections. The three magnetic reflections, that is, F-, A- and CE-types, seem to appear at the same temperature near T_{IM}. The F- and A-type (CE-type) components can be ascribed to the long-*c* (short-*c*) phase based on the lattice constants. The magnetic ordering at lower temperatures below T_{CO} *contradicts* to the percolation model. In addition, the volume ratio of the insulating short-*c* component rather decreases with cooling.

A new scenario for the insulator-metal behavior

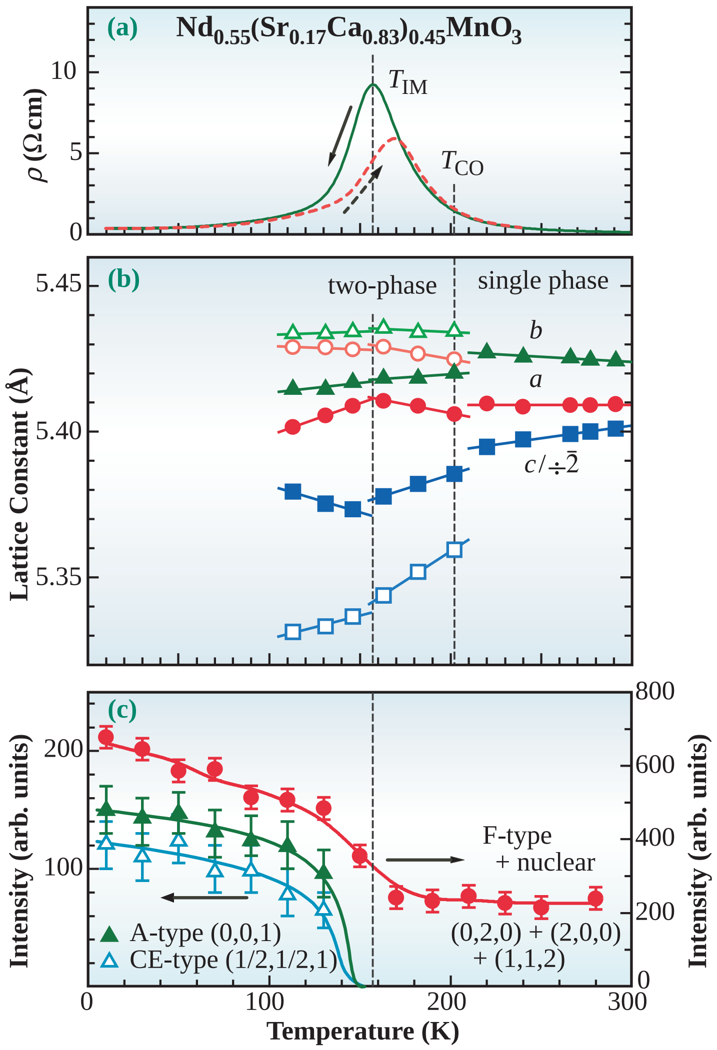

*Fig. 3. Temperature dependence of **(a)** resistivity ρ, **(b)** lattice constant and **(c)** intensity of the magnetic Bragg reflections of $Nd_{0.55}(Sr_{0.17}Ca_{0.83})_{0.45}MnO_3$. Open and closed symbols represent the short-c and long-c phases, respectively.*

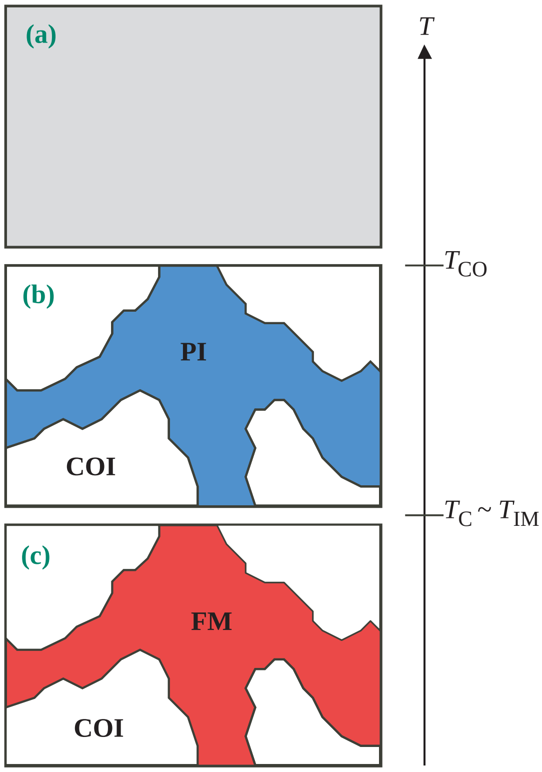

Fig. 4. Schematic illustrations of the mechanism for the insulator-metal behavior: ***(a)*** *$T > T_{CO}$,* ***(b)*** *$T_{IM} < T < T_{CO}$ and* ***(c)*** *$T < T_{IM}$. COI, PI and FM stand for the charge-ordered insulating, paramagnetic insulating and ferromagnetic metallic phases, respectively.*

is as follows. With a decrease in temperature below T_{CO}, the system is transformed from a single phase (Fig. 4(a)) to the two-phase state (Fig. 4(b)), possibly due to the stress-induced phase separation. These phases, that is, the short-*c* and long-*c* phases, can be ascribed to the COI and paramagnetic insulating (PI) phases, respectively. With further decrease of temperature below T_{IM}, the long-*c* phase indicates a PI to FM phase transition (Fig. 4(c)). If the metallic region were connected, the apparent insulator-metal transition would be observed.

Yutaka Moritomo and Akihiko Machida

Nagoya University

E-mail: moritomo@cirse.nagoya-u.ac.jp

References

[1] M. Uehara, *et al.*, Nature **399** (1999) 560.
[2] A. Machida, *et al.*, Phys. Rev. B **62** (2000) 3883.
[3] Y. Moritomo *et al.*, Phys. Rev. B **60** (1999) 10374.